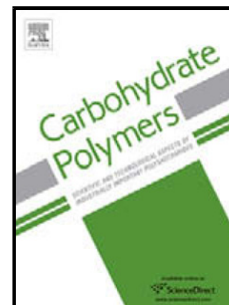


Accepted Manuscript

Title: Biophysical features of cereal endosperm that decrease starch digestibility

Authors: Laura Roman, Manuel Gomez, Cheng Li, Bruce R. Hamaker, Mario M. Martinez



PII: S0144-8617(17)30185-6
DOI: <http://dx.doi.org/doi:10.1016/j.carbpol.2017.02.055>
Reference: CARP 12034

To appear in:

Received date: 6-1-2017
Revised date: 11-2-2017
Accepted date: 14-2-2017

Please cite this article as: Roman, Laura., Gomez, Manuel., Li, Cheng., Hamaker, Bruce R., & Martinez, Mario M., Biophysical features of cereal endosperm that decrease starch digestibility. *Carbohydrate Polymers* <http://dx.doi.org/10.1016/j.carbpol.2017.02.055>

This is a PDF file of an unedited manuscript that has been accepted for publication. As a service to our customers we are providing this early version of the manuscript. The manuscript will undergo copyediting, typesetting, and review of the resulting proof before it is published in its final form. Please note that during the production process errors may be discovered which could affect the content, and all legal disclaimers that apply to the journal pertain.

Biophysical features of cereal endosperm that decrease starch digestibility

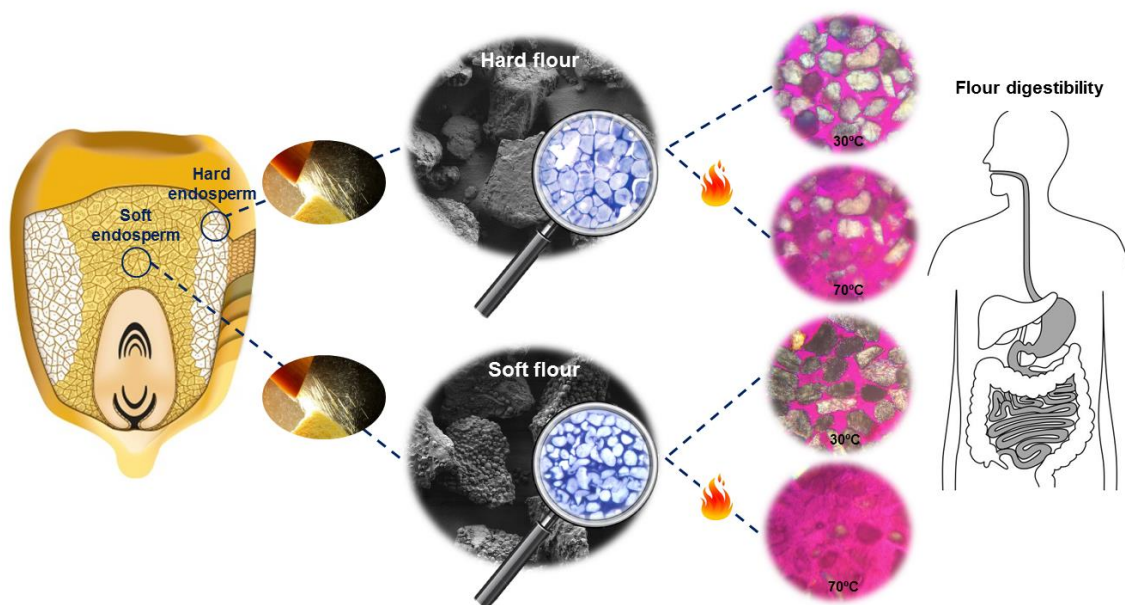
Laura Roman^{1,2}, Manuel Gomez¹, Cheng Li², Bruce R. Hamaker², Mario M. Martinez^{2*}

¹Food Technology Area. College of Agricultural Engineering, University of Valladolid, 34004 Palencia, Spain

²Whistler Center for Carbohydrate Research, Department of Food Science, Purdue University, 745 Agriculture Mall Drive, West Lafayette, IN 47907, USA.

*Corresponding author e-mail: mart1269@purdue.edu, mariomartinez175@gmail.com

Graphical abstract



Highlights

The effect of endosperm hardness on the digestibility of maize flours was studied

Hard endosperm resulted in flours with more peripheral damage within starch granules

Flours from hard endosperm were digested faster than soft counterparts before cooking

Flours from hard endosperm were digested slower than soft counterparts after cooking

The hard endosperm plant tissue matrix limited starch gelatinisation during cooking

Abstract

The influence of the physical structure of cereal endosperm on the natural structural integrity (intact cells) and starch bioaccessibility of the resultant flours was studied using maize as example. Endosperm hardness, defined by its intracellular (protein matrix) and extracellular (cell walls) constituents, affected the granular and molecular damage of the starch of the resultant flours leading to higher digestibility of raw hard than soft endosperm flours, but comparatively lower digestibility after cooking. After milling, hard endosperm possessed more damaged starch (radial splitting of amylopectin clusters) in the periphery of the resultant particles that increased *in vitro* starch digestibility of raw flours. Conversely, the hard endosperm plant tissue matrix significantly limited water availability and heat transfer on starch gelatinisation, thereby decreasing the digestion rate after hydrothermal processing (in particle size flours >80 μm). This study provides a unique mechanistic understanding to obtain cereal flours with slow digestion property for commercial utilisation.

Keywords: endosperm, maize, starch, digestion, flour, plant tissue, cell walls

1. Introduction

Diets containing a high proportion of foods with a low glycemic response (degree of blood glucose elevation after a meal) are associated with reduced risks of type 2 diabetes, heart disease or strokes (Jenkins et al., 2002; Wolever et al., 1992), and may also encourage weight loss (Brand-Miller, Holt, Pawlak, & McMillan, 2002). Maize (*Zea mays* L.) is a worldwide cultivated crop with multiple end-uses in the food industry. As with many other foods, maize-based products are mainly consumed in their plant tissue form, consisting of nutrients enclosed within plant cells (Edwards et al., 2015a), and are all reported as having high glycemic index (Foster-Powell, Holt, & Brand-Miller, 2002). Differences in glycemic response of foods depend highly on the rate and extent to which available starch is digested by α -amylase and made available for absorption in the small intestine after being fully digested by mucosal brush border α -glucosidases (Jenkins et al., 1982; Lee et al., 2013).

In 2015, Edwards et al. (2015a) provided the first evidence that the structural integrity of endosperm is a major factor in influencing starch bioaccessibility [defined as proportion of starch that is potentially available for absorption in the small intestine (Parada, & Aguilera 2007; Grundy et al. 2016)], and that manipulating the structural integrity of the endosperm has the potential to significantly influence postprandial glycaemia and metabolism. Maize endosperm is comprised of a large number of cells, each packed with starch granules embedded in a continuous matrix of protein; all the cell contents are surrounded by a cell wall (Eckhoff, & Watson, 2009). Mature endosperm of dent maize contains a central core of soft or floury endosperm extending to the crown and surrounded by a glassy-appearing region known as horny or hard endosperm. The average ratio of floury to horny regions is about 1:2. The floury region is characterized by larger cells, large spherical starch granules and a relatively thin

protein matrix. On the other hand, in the horny endosperm, granules are closely-packed and the protein content is slightly higher (1.5-2.0 % higher) (Eckhoff, & Watson, 2009). These biophysical features define the endosperm hardness and therefore its behavior during milling, which may affect not only the degree of integrity of starch (Morrison, Tester, & Gidley, 1994; Tran et al., 2011), but also of the plant tissue matrix. Understanding the mechanisms of edible plant tissue damage during milling and its relationship with starch digestibility of the resultant flours may suggest ways of manipulating existing foods and/or ingredients to control metabolic responses.

In the last decade, several authors have reported that coarse particles are digested slower than their fine counterparts, thereby decreasing the glycemic response of milled grains (Al-Rabadi, Gilbert, & Gidley, 2009), porridges (Edwards et al., 2015a) and breads (de la Hera, Rosell, & Gomez, 2014). However, coarse flours do not always meet functional criteria set by the industry and are not suitable for the manufacturing of certain foods, such as cakes (de la Hera, Martinez, Oliete, & Gomez, 2013a; Dhen, Román, Rejeb, Martínez, Garogouri, & Gómez, 2016; Segundo, Román, Gomez, & Martinez, 2017). Therefore, finding alternative ways to decrease starch bioaccessibility other than increasing the particle size would provide the opportunity to develop novel ingredients with potential applications in the management and prevention of hyperglycemia-related diseases.

The objective of this study was to provide a mechanistic understanding of the influence of the biophysical features of maize endosperm on its macro- and microstructural mechanical damage during milling and on digestibility of the resultant flours. We hypothesized that both the plant tissue matrix and extent of starch damage influence the digestibility of native and cooked flours with the same particle size. This unique study

provides a new insight into the selection of cereal endosperm tissue with optimum biophysical features to manufacture flours for foods with low glycemic response.

2. Materials and Methods

2.1 Materials

Yellow dent maize was industrially decorticated to remove its bran and germ fractions and subsequently roller-milled and sieved at the milling company DACSA (Valencia, Spain). The initial breakage of the maize endosperm gave rise to three fractions depending on its hardness. The intermediate fraction, which consisted mainly of grits smaller than 2 mm and semolina ($>250\ \mu\text{m}$), was discarded. The largest (grits larger than 2 mm) and the smallest (flour that passed through a sieve of $250\ \mu\text{m}$ and termed in this study as soft flour) fractions were collected, representing the candidates for the hard and soft fractions of the endosperm, respectively. This was microscopically evidenced by their different degrees of granular compactness (Fig. 1).

Grits were further re-milled into flour (termed in this study as hard flour) in a LM 3100 hammer mill (Perten Instruments, Sweden). Subsequently, both hard and soft flours were sieved in a Bühler MLI300B automatic sieve (Bühler, Braunschweig, Germany) for 25 min using screens of 80, 130 and $180\ \mu\text{m}$ obtaining three fractions: fine ($<80\ \mu\text{m}$), medium ($80\text{-}130\ \mu\text{m}$) and coarse ($130\text{-}180\ \mu\text{m}$). The flow chart of flour production with the moisture and protein content of each flour is shown in Fig. S1. Flours were stored at room temperature separately in plastic sealed bags until further analyses.

Protease from *Streptomyces griseus* (type XIV) and α -amylase from porcine pancreas (A3176) were purchased from Sigma-Aldrich (St Louis, MO, USA). Dimethyl sulfoxide (DMSO, GR for analysis ACS) and lithium bromide (ReagentPlus) were purchased from VWR (Radnor, PA, USA) and Beantown Chemical (Hudson, NH, USA),

respectively. A damaged starch assay kit and isoamylase from *Pseudomonas* sp. were purchased from Megazyme International Ltd. (Co. Wicklow, Ireland).

2.2. Methods

2.2.1. Particle size distribution, damaged starch, moisture and protein content

Flours were analyzed following AACC Methods (AACC, 2015) for moisture (44-16.01), damaged starch (76-31.01) and protein (46-30.01) with a Leco TruSpec device (Leco, St. Joseph, MI, USA). The particle size of each was measured with a laser diffraction particle size analyser Mastersizer 3000 (Malvern Instruments, Worcestershire, UK) and the particle size distribution for each fraction is shown in Fig. S2.

2.2.2. Microscopy

For examination by light microscopy, flours were fixed in 2.5 % glutaraldehyde at 4 °C for 24h, rinsed with 0.1 M sodium cacodylate buffer (pH 7.4), fixed in 1 % osmium tetroxide with 0.8 % potassium ferrocyanide for 2 h at room temperature and rinsed with water. Samples were then dehydrated using increasing concentrations of ethanol. Samples from hard endosperm were infiltrated with freshly prepared LR White Acrylic resin (London resin company Ltd, Reading, Berkshire, England) and polymerized in gelatin capsules by UV light at room temperature for 48 h. On the other hand, samples from soft endosperm, which did not resist the former conditions, were infiltrated in a rotator mixer with a mixture of acetonitrile and Embed 812 epoxy resin (Electron Microscopy Sciences, Hatfield, PA, USA) in 2:1 and 1:2 ratios at 60 °C for 2 h and overnight, respectively. The cured samples (both from hard and soft endosperm) were trimmed and sectioned (0.5µm) on an Ultracut E, Reichert-Jung ultra-microtome mounted with a diamond knife. Sections were stained with toluidine blue (1 %, w/v, with 1 %, w/v, sodium borate) and viewed on an Olympus BH-2 light microscope

(Olympus, Tokyo, Japan). Images were captured with a SPOT Insight Wide-field digital camera and Spot microscope software.

For scanning electron microscopy, flours were pictured with a Quanta 200FEI (Hillsboro, Oregon, USA) ESEM in beam deceleration mode (BDM) at 1.5 KeV in high vacuum mode with a backscattered electron detector (BSED).

The swelling and loss of birefringence of the starch from the coarse fraction (130-180 μm) of soft and hard flours were analysed under an Omano polarizing light microscope (Omano, China) equipped with a hot stage during heating from 30 °C to 90 °C. Photos were taken using an iPhone 5 camera attached by an iDu Microscope Adapter.

2.2.3. Flour crystallinity by X-ray diffraction (XRD)

Samples were analysed using a Shimadzu 6000 X-ray Diffractometer (Shimadzu) operating at 40 kV and 30 mA, producing CuK α radiation of 0.154nm wavelength. Diffractograms were obtained by scanning from 3 ° to 40 ° (2theta) at a rate of 2 °/min. Relative crystallinity was calculated as the sum of the area of each crystalline peak divided by the total area (both crystalline peaks and amorphous background) using Origin pro 2016 (Origin lab corporation, Northampton, MA, USA.).

2.2.4. Thermal properties of maize flours

Analyses were performed in a differential scanning calorimeter Q-20 (TA instruments, Crawley, UK) equipped with a refrigerated cooling system (RCS 40). Prior to sample measurements, the calibration for enthalpy and temperature was completed using indium ($T_{\text{onset}} = 155.74$ °C and $\Delta H = 28.69$ J/g). Tzero hermetic aluminum DSC pans (TA-Instruments) were employed. An empty pan was used as reference and dry nitrogen at a flow rate of 50 mL/min was used as the purge gas. Flour (6 mg) was loaded into the aluminum pan and distilled water (18 μL) was added using a micro syringe. Samples were hermetically sealed and allowed to equilibrate for 60 min at 30 °C before heating

in the DSC oven. Samples were kept at 30 °C for 2 min, heated from 30 to 100 °C at 10 °C/min. Onset temperature (T_o), peak temperature (T_p), conclusion temperature (T_c) as well as the enthalpy (ΔH_g) (expressed as J/g of sample in dry basis) of starch gelatinization were determined. All samples were run in triplicate.

2.2.5. Size-exclusion chromatography (SEC)

For molecular size distribution of (whole) fully branched starch, starch was extracted from maize flour and dissolved in DMSO solution containing lithium bromide (0.5 % w/w) (DMSO/LiBr). For molecular size distribution of individual branches of starch molecules, starch was extracted from a larger amount of maize flour (~5 mg) using the same method as described for the sample preparation of fully branched starch. The extracted starch in 1 mL of DMSO/LiBr solution was precipitated with 3mL of absolute ethanol and then debranched using isoamylase (Hasjim, Cesbron Lavau, Gidley, & Gilbert, 2010).

The molecular size distributions of fully branched and debranched starches from maize flour were analysed in duplicate using a size exclusion chromatography (SEC) system (Agilent 1260 series, Agilent Technologies, Waldbronn, Germany) equipped with a refractive index detector (RID, RID-10A, Shimadzu, Kyoto, Japan) (Tran et al., 2011). The size distribution was plotted as SEC weight distribution, $w(\log V_h)$, derived from RID signals against hydrodynamic radius, R_h . The degree of polymerization (DP) of linear branches was calculated from the V_h using the Mark-Houwink equation (Vilaplana, & Gilbert, 2010a). While this approach is not especially accurate, we are primarily interested in relative changes; small errors in the absolute values will make no qualitative difference to the overall conclusions.

The average hydrodynamic radius (R_h) of whole starch molecules was calculated following the methods detailed by Vilaplana and Gilbert (2010b). The fine molecular

structures of amylopectin (Ap) and amylose (Am) branches are reported as the DP at each peak maximum (two for amylopectin peaks denoted by X_{Ap1} and X_{Ap2} , and one for amylose peak denoted by X_{Am1}) and the peak height of each peak maximum is reported as the ratio to the height of the first amylopectin peak maximum (denoted by $h_{Ap2/Ap1}$, $h_{Am/Ap1}$). The Am content of maize starch was determined from the SEC weight molecular size distribution of debranched starch as the ratio of the area under the curve (AUC) of Am branches to the AUC of overall Ap and Am branches (International Standardization Organization, 2011; Vilaplana, Hasjim, & Gilbert, 2012).

2.2.6. Viscosity profile of flours during a heating cycle

The viscosity profile of flours was determined following the AACC standard method 61.02.01 (AACC, 2015) using a Rapid Visco Analyser (RVA-4C) controlled by Thermocline software (Perten, Uppsala, Sweden) for Windows. RVA measurements were carried out in duplicate.

2.2.7. *In vitro* starch digestibility

The rate at which starch amylolysis products become bioaccessible (i.e., available for absorption) during digestion in the small intestine is an important determinant of the duration and magnitude of the glycemic response. Because of the difficulty in studying luminal digestion of starch *in vivo*, the rate and extent of starch amylolysis in the different flours was determined *in vitro* with the use of a method involving sample digestion with porcine pancreatic α -amylase and the quantification of digestion products through the determination of reducing sugars. Enzymatic digestion of native endospermic samples was carried out using 3.7 unit of porcine pancreatic α -amylase (Sigma A6255) per mg of starch. Starch (50 mg) was suspended in 10mL of MOPS buffer (50 mM, pH 7) containing 0.02 % (w/v) sodium azide and calcium chloride (5 mM). The mixture was incubated at 37°C with constant stirring at 350 rpm with a 3 mm

× 6 mm magnetic stirrer bar. At defined time intervals, 50 µL of aliquot was immediately boiled at 100 °C to stop the enzymatic reaction. The supernatant was used to determine the reducing sugar content using the DNS method (Miller, 1959). Only the first 60 min of amylolysis was assayed, as this provided sufficient information for the application of the different kinetic models. To test for endogenous reducing sugars or enzyme activity, the addition of amylase was omitted for control assays, showing that the amount of reducing sugar freshly produced in these controls was undetectable. Cooked samples were analyzed as before but with a hydrothermal process at 100 °C for 20min with gentle stirring prior to digestion using 0.36 unit porcine pancreatic α -amylase per mg of starch. Increasing the concentration of amylase in native samples enhanced the reaction rate improving the precision of rate measurements. Tests were run in triplicate.

Starch amylolysis data of cooked fractions were fitted to a pseudo-first-order equation (Goñi, Garcia-Alonso, & Saura-Calixto, 1997):

$$C_t = C_\infty(1 - e^{-kt}) \text{ eq. 1}$$

where C_t is the concentration of product at a given time (t), C_∞ is the concentration of product at the end of the reaction, and k is the digestibility rate constant. However, starch amylolysis data from native fractions did not follow the classic exponential model since the digestion rate constant was not constant over time. In order to study the different digestion rates at different times, a Logarithm of Slope (LOS) plot was obtained by expressing the first derivative of the first-order equation in logarithmic form (eq. (2)) as in Edwards et al. (2014). This gives a linear plot in which the values of digestibility constants, k and C_∞ , are calculated from the slope ($-k$) and y-intercept ($\ln[C_\infty k]$), respectively.

$$\ln\left(\frac{\partial C}{\partial t}\right) = -kt + \ln(C_\infty k) \text{ eq. 2}$$

2.2.8. Statistical analysis

Differences among results were studied by analysis of variance (one-way ANOVA). Fisher's least significant difference (LSD) was used to describe means with 95 % confidence intervals. The statistical analysis was performed with the Statgraphics Centurion XVI software (Statpoint Technologies, Inc., Warrenton, USA).

3. Results and discussion

3.1 Flour microstructure

Micrographs confirmed that for each sieved fraction, flours with different compactness were obtained (Fig.1 A-F). For each of the particle sizes, flours from hard endosperm (A-C) exhibited a smooth or plain superficial appearance, which may suggest that starch granules are more tightly aggregated or more embedded/covered by the protein matrix. Conversely, starch granules in flours from soft endosperm (D-F) were loosely packed, resulting in less compact flour particles (see higher magnification micrographs in Fig. 1C, F). Other authors have reported a higher degree of granular compactness in hard maize endosperm than in the soft counterpart, the latter having more intergranular spaces (Narváez-González, Figueroa-Cárdenas, Taba, & Rincón-Sánchez, 2006). This has also been evidenced in other cereals, such as rice, where flours from long grain rice presented a more compact and vitreous endosperm (de la Hera, Gomez, & Rosell, 2013b). Thus, we expect that the results of this work can also be extended to the manufacturing of other cereal plant tissue-based ingredients.

Light microscopy (Fig. G and H) also confirmed the greater close-packed granular conformation of the hard endosperm flour. Conversely, soft flours presented air pockets (arrow a), which have been attributed to the rupture of the thin strands of protein matrix during kernel drying, giving the soft endosperm a porous texture (Wang, & Eckhoff, 2000). This is in agreement with the lower protein content found in flours from soft endosperm (Fig. S1). Both endosperms displayed starch granules with similar amount of interior channels (arrow b, Figs. G and H). Hard flours possessed a higher amylose content (Table 1), which has been reported to induce starch granule-granule adhesion and compression of the endosperm (Dombrink-Kurtzman, & Knutson, 1997; Jiang et al., 2010). Moreover, at lower magnification (Fig. I and J), light microscopy also revealed that the hard flour contains smaller sized cells compared to soft flour, indicating a higher amount of cell walls (arrow c) with more physically restricted granules. Cells walls in cereals are categorized as “type II”, based on their polysaccharide composition. Type II cell walls are characterized by cellulose microfibrils cross-linked by glucuronoarabinoxylans. In particular, maize also contains mixed-linkage (1, 3) - (1, 4)- β -D-glucans (called β -glucans, Carpita et al., 2001).

The aforementioned granular compactness, amylose content, protein content and thicker protein matrix, and the amount of cell walls in hard endosperm results in flours with greater adherence of cell constituents contributing to higher physical resistance of the endosperm to milling (Juarez-García, Agama-Acevedo, Gomez-Montiel, Pando-Robles, & Bello-Perez, 2013).

3.2. Damaged starch and short and long-range molecular order

The amount of damaged starch was higher in hard flours and increased with a reduction in particle size (Table 1). Milling of hard endosperm grains resulted in higher damage to the starch granules than soft grain-milling, as other authors also reported (Li, Dhital, &

Hasjim, 2014). This is due to the greater amount of mechanical energy required to break the structure of hard grains. As for the particle size, there are contradictory studies showing that higher amount of damaged starch can be present in fine (Tran et al., 2011) and coarse rice flours (de la Hera et al., 2013a). The former authors modified the screen opening, forcing the small particles to be inside the mill for a longer duration, and thereby exposing them to more mechanical energy. However, the latter kept the screen size constant and observed the opposite effect. In order to obtain deeper understanding of those occurrences, the loss of short- (amylopectin double helices) and long- (crystalline structures) range molecular order of starch was analyzed.

The melting of double helices of starch chains was evaluated through DSC (Table 1). Starch gelatinization entails a disruption of the amylopectin double helices resulting in an endothermic transition. Hard flours were characterized by lower temperature at onset of gelatinization (T_o) than soft counterparts. T_o of starch granules reflects the heat stability of those double helices more accessible to heat (Hasjim, Li, & Dhital, 2013). Therefore, the mechanical damage during milling may increase the number of double helices that are more exposed to the heat and water, an occurrence that is independent of the particle size. In fact, it is known that damaged starch granules, containing a partially disrupted crystalline structure, have lower T_o than intact starch granules (Dhital, Shrestha, Flanagan, Hasjim, & Gidley, 2011; Morrison et al., 1994). Since damaged granules are located predominantly at the surface of flour particles, the inner part of the particle stays relatively intact (Hasjim et al., 2013), and this is likely the reason why T_p and T_c were not affected by the endosperm hardness. However, significantly higher values of T_c were only found for coarse hard flours. T_c of starch granules represents the heat stability of those double helices that are less accessible to heat, i.e., those in the inner part of the particle. The denser plant tissue matrix of hard flours (non-starch intra-

and extracellular components) may limit heat and water transfer in flours larger than a certain particle size (coarse flours), which may increase the stability of double helices in the inner parts of the particles. T_c was reduced with a decrease in particle size, which may be logical considering the lesser amount of inner double helices that are less accessible to heat when particle diameter is reduced, i.e., less distance for the heat at the surface of the particle to reach the inner starch double helices through convective mechanism. In fact, Hasjim et al. (2013) found that T_c of coarse rice flours was significantly higher than that of fine flours after hammer-milling. Enthalpy, representing the amount of double helices, was lower for hard than soft flours. A similar trend was reported by Narvaez-Gonzalez et al. (2006), where hard maize kernels were found to have a lower gelatinization enthalpy than soft kernels. This may be associated with a lower amount of amylopectin external chains (higher $H_{Am/Ap1}$, Table 2), which are precursors of the thin crystalline lamella through the formation of double helices (Li, Blanco, & Jane, 2007). Accounting for the fact that no differences in enthalpy were found for particle size, in contrast to the differences found for damaged starch, it is suggested that the mechanical damage during milling does not disrupt amylopectin double helices.

Parallel double helices of A and B amylopectin chains can assemble into radially-oriented clusters forming a “shell” of ordered material, whose crystalline order can be measured by X-ray diffraction. In fact, the positive birefringence of native starch indicates a radial orientation of the principal axis of the crystallites (Morrison et al. 1994; Perez, Baldwin and Gallant, 2009). Morrison et al. (1994) reported that the primary event caused by mechanical damage, through studying ball-milled maize starch, is the conversion of large ordered regions into essentially disordered amorphous material. In particular, these authors reported a radial splitting of the weaker helical

aggregates displacing clusters, and eventually leading to separation of helices. This is something that must be considered important from a digestibility standpoint, since it makes the starch freely accessible to water and amylolytic enzymes. In order to confirm the radial splitting of the helical aggregates, the relative crystallinity (long-range molecular order) of flours was also analyzed (Table 1). All flours contained starch with the A-type diffraction pattern typical for cereals (data not shown) and with relative crystallinity ranging from 15.99 to 23.01 % (Table 1). XRD results showed a lower crystallinity for hard flours, which may confirm the separation of double helical aggregates within the crystalline lamellae and therefore a loss of crystalline order. Since the damage is thought to be peripheral, the lower surface area of coarse particles may be responsible for diluting these differences. The relative crystallinity did not significantly vary with the particle size, although, in soft flours, the coarse fraction possessed lower relative crystallinity.

Overall, the results suggest that the highest hardness of hard flours increased the mechanical energy necessary to break the endosperm which resulted in flour particles with more damaged granules in their periphery. These results also indicate that the physical damage was produced at the level of the crystalline lamellae, consisting of radial splitting and separation of double-helical crystalline aggregates.

3.3. Starch fine molecular structure

The molecular size distributions of debranched and native starch polymers were characterized using SEC. All SEC weight distributions were normalized to yield the same height of the highest peak to bring out detailed features and to facilitate qualitative comparison and interpretation (Fig. 2). Typical chain length distributions of debranched starch molecules (Fig. 2A) shows bimodal peaks representing amylopectin branches (single-lamella, peak $R_h \sim 1.5$ nm or $DP \sim 16$; trans-lamella, R_h peak ~ 2.5 nm, $DP \sim 50$)

and amylose branches ($R_h \sim 5\text{--}80$ nm, $DP \sim 100\text{--}10,000$) (Wang, Hasjim, Wu, Henry, & Gilbert, 2014). The main structural parameters are summarized in Table 2. No significant differences were found in the chain length distributions of amylopectin, except for minor differences in X_{Ap1} and X_{Am} for the coarsest fraction of soft flours. Li et al. (2014) reported that degraded amylopectin molecules in many cereal grains do not show apparent changes in their branch-chain length distributions after milling. On the other hand, the ratio of long to short amylopectin branches ($H_{Ap2/Ap1}$) was lower in hard flours, indicating a lower number of internal longer chains. As it was reported in the previous section, hard endosperm requires more mechanical energy to break its macromolecular structure to attain desired particle size. Therefore, it seems that the internal chains of amylopectin (amylopectin fine structure) may be broken, decreasing $H_{Ap2/Ap1}$, an effect that is minimized with the manufacture of coarse flours. Meanwhile, soft flours presented a lower ratio of amylose to short amylopectin branches ($H_{Am/Ap1}$). The amylose chain length from soft flours was higher than amylose from hard flours.

The branched SEC weight distribution of starch from flours (see Fig. 2B) exhibits two distinct peaks for amylose and amylopectin molecules separated at $R_h \sim 40$ nm. Hard flours presented amylopectin with lower R_{hAp} than the soft counterparts (although significant differences were only found in the coarse fractions). Morrison and Tester (1994) also observed a reduction in the molecular weight of amylopectin when samples were ball-milled. The higher amylose peaks in the molecular size distributions of the native starch indicate that the fragmented amylopectin molecules are co-eluting with amylose, suggesting that the cleavage occurs in the inner part of the amylopectin molecule, resulting in degraded amylopectin with hydrodynamic size within the range of that of amylose. This occurrence has been also reported by Tran et al. (2011) after

hammer-milling of rice kernels. Even though there was significant molecular fragmentation in both studies, fine structures were not altered as measured by debranched chain length distribution.

Milling of hard endosperm grain resulted in reduced size of amylose (X_{Am} and R_{hAm}). Tran et al. (2011) also reported a decrease in the amount of long amylose chains during the hammer-milling of rice grains. These authors suggested that hammer-milling was more likely to cleave longer chains, given that they are more susceptible to mechanical forces as they span through more than one less-rigid amorphous lamella. Overall, endosperm hardness affected the starch damage not only at high hierarchical levels of structure, but also at the molecular level.

3.4. Limitations of starch gelatinization: RVA and hot-stage polarized microscopy

The limitations of starch swelling and gelatinization imposed by the plant tissue matrix were analyzed through the development of viscosity and loss of birefringence during heating. The pasting properties of hard and soft flours are depicted in Figure 3. During heating, water de-stabilizes hydrogen bonds in the amorphous regions of the starch granules, enabling further water ingress which is accompanied by granular swelling. Flours with coarse particle size presented a more delayed and restricted granular swelling, as their higher pasting temperature and lower peak viscosity indicated. This can be attributed to the lower surface area and damaged starch, restricting water diffusion and swelling. Edwards et al. (2015a,b) pointed out that the effect of particle size on gelatinization behavior is not simply a result of available surface area, but also of the integrity of the physical structure that encapsulates the starch, e.g. plant cell walls. This could explain the differences found regarding flour compactness, where hard flours displayed a higher pasting temperature and a lower peak viscosity. This would indicate that the more compact plant tissue matrix of hard flours (section 3.1) would

restrict water uptake of the starch granules which delays gelatinization. Narvaez-Gonzalez et al. (2006) indicated that the lack of intergranular spaces in maize hard endosperm limits water's ability to diffuse easily into that material and decreases water absorption. This effect was less noticeable in fine fractions, where the higher surface area of fine flours may mask the flour matrix effect on the pasting profile. It is also noteworthy that amylopectin is the main molecule associated with swelling. Therefore, a lower viscosity profile is also expected for hard flours according to their higher molecular damage produced during milling, which may lead to a granular weakening that increases the cooking loss and reduces the water uptake. The reinforcement effect of the endosperm matrix (section 3.1) on hard and coarse flours also became evident after reaching gelatinization temperatures, as indicated by the lower breakdown (viscosity decline after the peak viscosity). In this way, coarse or hard flours were more resistant to disintegration under shear stress after gelatinization. Li et al. (2014) have already highlighted the abilities of native protein and cell-wall matrices in flour to stabilize the flour paste and to prevent the rupture of swollen starch granules during heating with shearing. Furthermore, Shi et al. (2016) have also stated that the higher breakdown found in fine flours is due to the greater ability of swollen starch granules to disintegrate when reducing particle size.

During cooling of gelatinized starch, hydrogen bonds develop between the amylose chains, creating a new crystalline structure that pushes out the absorbed water, causing a renewed increase in viscosity (setback), a phenomenon known as retrogradation. During this phase, the α -glucan chains organize into a tightly packed crystalline structure. Setback was more evident in soft flours compared to the hard counterparts, which may be attributed to their longer amylose molecules (higher X_{Am}), which are more prone to

form small aggregates of amylose double helices (junction zones) that increase paste viscosity (Biliaderis, 2009).

The effect of the plant tissue matrix on the loss of starch birefringence during heating was assessed through hot-stage polarized microscopy (Figure 4). When native starch granules are observed under polarized light, they show birefringence, indicating the presence of ordered structures. During heating in excess of water, starch gelatinization occurs, which is accompanied by a loss of birefringence as the starch becomes more amorphous (Donovan, 1979). These events are shown in Fig 4. At 70 °C, most of the starch granules contained in soft flour particles lost their birefringence and swelled, whereas granules contained in the hard flour matrix swelled less and preserved their birefringence. This confirms that the plant tissue matrix had a major effect on the preservation of the starch molecular order during heating. Dhital, Bhattarai, Gorham, and Gidley (2016) and Edwards et al. (2015b) also highlighted the role of an intact cell

3.5. Starch digestibility of native and hydrothermally-processed maize flours

Native maize flours were not digested following the classical pseudo-first order kinetics, but two amyolysis phases were observed. The curves were fit to the LOS model described by Edwards et al. (2014) and the parameters are shown in Table 3. Curves were characterized by an initial linear step with a significantly higher rate constant (k_1 , corresponding to the digestion rate of readily accessible starch), followed by a linear step with a significantly smaller rate constant (k_2 , corresponding to less accessible starch). Dhital, Shrestha, and Gidley (2010) proposed that once the enzyme penetrates into the inner part of the granule, more time is required for the enzyme to diffuse and hydrolyze the less accessible starch, leading to a decrease in the k_2 rate constant. In the present study, k_2 was roughly 20% slower than k_1 . An example of a digestion curve is shown in Fig. S3. Hard flours presented higher k_1 and k_2 than soft

flours, except for coarse particle size flours, where no significant differences were found. In the case of k_2 , only significant differences were found for the intermediate particle sizes. Added to that, hard flours were hydrolyzed to a greater extent than the soft ones, as represented by a higher C_∞ .

As mentioned before, hard flours suffered from more mechanical damage during milling as a consequence of plant tissue hardness, resulting in a greater amount of damaged starch (Table 1). It seems that more granular damage (see section 3.2) may result in more access points for the digestive enzymes to bind the starch and, therefore, increase its bioaccessibility. However, at larger sizes, despite a significantly higher amount of damaged starch in hard flour, differences in the digestion rates became negligible, suggesting an effect of the flour matrix on decreasing enzyme permeability throughout the particle. As for the particle size, as expected, coarser flours possessed lower k_1 , indicating a lower digestion rate of the readily accessible starch. However, no significant differences were found for the digestion rate of the less accessible starch. Several authors have already reported a lower digestion rate for coarse particles (Al-Rabadi et al., 2009; de la Hera et al., 2014; Edwards et al., 2015a). As mentioned before, fine particles have a higher amount of peripheral damaged starch and surface area, facilitating the enzyme binding to the readily accessible starch.

In many food products, conventional hydrothermal processing promotes partial or complete starch gelatinization. This is the case for white bread, yellow cake or sugar cookie, with gelatinized starch content of 70, 75 and 11 % (in bread and cake measured in the center of the crumb) (Varriano-Marston, Ke, Huang, & Ponte, 1980). The amorphous structure of gelatinized starch results in a greater availability of α -amylase binding sites, which makes the substrate more susceptible to enzyme hydrolysis (Baldwin et al., 2015). Considering the vast differences in digestion rate between native

and gelatinized starches, partial gelatinization would be expected to have major implications for digestibility and postprandial glycaemia. The digestion kinetics of all samples followed one single step of the digestion reaction (Fig. S4) and data was fitted to an exponential equation defined by a unique rate constant (k) (Table 3). In contrast to the results reported for native flours, fine and medium hard flours did not have a significantly different digestion rate from soft flours. Moreover, in coarse particles, a significantly lower digestion rate was found for hard flours. As mentioned in section 3.4, the plant tissue matrix had a major effect on the preservation of the starch molecular order during heating. Thereby, intracellular (protein matrix) and extracellular components (cell walls) of endosperm may restrict starch gelatinization during cooking to a major extent, limiting the heat, water or space required for granular swelling. Furthermore, it has been reported that the presence of some intact cell walls in legumes after cooking can provide a physical barrier to the diffusion of enzymes inside the cells, controlling the hydrolysis of starch (Dhital et al., 2016). As for particle size, coarse flours (both hard and soft flours) were also digested at slower digestion rate than fine flours, with no significant differences in the extent of digestion (C_{∞}). This may be attributed not only to the major effect of the plant tissue matrix after cooking in coarse flours, but also to their smaller surface area that may hinder starch-enzyme binding. This was reported by Martinez, Calvino, Rosell, & Gomez, 2014), where coarse flours were digested slower than soft flours in a fully gelatinized state attained by extrusion.

4. Conclusions

The food and ingredient industries are seeking ways to optimize manufacturing of edible plant tissues with a low glycaemic response. This objective becomes especially challenging when the food system undergoes total or partial starch gelatinisation, both having major implications for digestibility and postprandial glycaemia. In this work, we

provide a unique insight of the influence of the biophysical features of cereal maize endosperm on the cellular integrity of the resultant flours after milling and their digestibility. Furthermore, this study serves as starting point for the application of edible plant tissues with specific macromolecular physical structure in different food systems. Since starch is a major energy-providing carbohydrate for humans, we envision that this work is highly relevant to the development of novel ingredients and functional foods, with potential applications in the prevention of cardiometabolic diseases and obesity.

5. Acknowledgements

Laura Roman would like to thank the visiting scholar program of the University of Valladolid that allowed her to complete a research stay at Purdue University under the supervision of Mario M. Martinez and Bruce R. Hamaker.

6. References

AACC (2015) *Approved methods of the American Association of Cereal Chemists*, for moisture (44-16.01), damaged starch (76-31.01), protein (46-30.01) and pasting properties (61-02.01), 11th ed., St. Paul, Minnesota, American Association of Cereal Chemists.

Al-Rabadi, G. J. S., Gilbert, R. G., & Gidley, M. J. (2009). Effect of particle size on kinetics of starch digestion in milled barley and sorghum grains by porcine alpha-amylase. *Journal of Cereal Science*, 50, 198-204.

Baldwin, A. J., Egan, D. L., Warren, F. J., Barker, P. D., Dobson, C. M., Butterworth P. J., & Ellis, P.R. (2015). Investigating the mechanisms of amylolysis of starch granules by solution-state NMR. *Biomacromolecules*, 16, 1614–1621.

Biliaderis, C. G. (2009). Structural transitions and related physical properties of starch. In: J. BeMiller, & R. Whistler (Eds.), *Starch. Chemistry and Technology* (pp. 293-372). New York: Academic Press.

Brand-Miller, J. C., Holt, S. H., Pawlak, D. B., & McMillan, J. (2002). Glycemic index and obesity. *American Journal of Clinical Nutrition*, 76, 281S–285S.

Carpita, N. C., Defernez, M., Findlay, K., Wells, B., Shoue, D. A., Catchpole, G., Wilson, R. H., & McCann, M. C. (2001). Cell wall architecture of the elongating maize coleoptile. *Plant Physiology*, 127, 551-565.

de la Hera, E., Gomez, M., & Rosell, C. M. (2013b). Particle size distribution of rice flour affecting the starch enzymatic hydrolysis and hydration properties. *Carbohydrate Polymers*, 98, 421-427.

de la Hera, E., Martinez, M. M., Oliete, B., & Gomez, M. (2013a). Influence of flour particle size on quality of gluten-free rice-cakes. *Food and Bioprocess Technology*, 6, 2280-2288.

- de la Hera, E., Rosell, C. M., & Gomez, M. (2014). Effect of water content and flour particle size on gluten-free bread quality and digestibility. *Food Chemistry*, 151, 526-531.
- Dhen, N., Román, L., Rejeb, I. B., Martínez, M. M., Garogouri, M., & Gómez, M. (2016). Particle size distribution of soy flour affecting the quality of enriched gluten-free cakes. *LWT - Food Science & Technology*, 66, 179-185.
- Dhital, S., Bhattarai, R. R., Gorham, J., & Gidley, M. J. (2016). Intactness of cell wall structure controls the in vitro digestion of starch in legumes. *Food & Function*, 7, 1367-1379.
- Dhital, S., Shrestha, A. K., & Gidley, M. J. (2010). Relationship between granule size and in vitro digestibility of maize and potato starches. *Carbohydrate Polymers*, 82, 480-488.
- Dhital, S., Shrestha, A. K., Flanagan, B. M., Hasjim, J., & Gidley, M. J. (2011). Cryomilling of starch granules leads to differential effects on molecular size and conformation. *Carbohydrate Polymers*, 84, 1133-1140.
- Dombrink-Kurtzman, M. A., & Knutson, C. A. (1997). A study of maize endosperm hardness in relation to amylose content and susceptibility to damage. *Cereal Chemistry*, 74, 776-780.
- Donovan, J. W. (1979). Phase transitions of the starch-water system. *Biopolymers*, 18, 263-275.
- Eckhoff, S. R., & Watson, S. A. (2009). Corn and sorghum starches: Production. In: J. BeMiller, & R. Whistler (Eds.), *Starch. Chemistry and Technology* (pp. 373-439). New York: Academic Press.
- Edwards, C. H., Grundy, M. M. L., Grassby, T., Vasilopoulou, D., Frost, G. S., Butterworth, P. J., Berry, S. E. E., Sanderson, J., & Ellis, P. R. (2015a). Manipulation

of starch bioaccessibility in wheat endosperm to regulate starch digestion, postprandial glycemia, insulinemia, and gut hormone responses: a randomized controlled trial in healthy ileostomy participants. *American Journal of Clinical Nutrition*, 102, 791-800.

Edwards, C. H., Warren, F. J., Campbell, G. M., Gaisford, S., Royall, P. G., Butterworth, P. J., & Ellis, P. R. (2015b). A study of starch gelatinisation behaviour in hydrothermally-processed plant food tissues and implications for in vitro digestibility. *Food & Function*. 6, 3634-3641.

Edwards, C. H., Warren, F. J., Milligan, P. J., Butterworth, P. J., & Ellis, P. R. (2014). A novel method for classifying starch digestion by modelling the amylolysis of plant foods using first-order enzyme kinetic principles. *Food & Function*, 5, 2751-2758.

Foster-Powell, K., Holt, S. H., & Brand-Miller, J. C. (2002). International table of glycemic index and glycemic load values: 2002. *American Journal of Clinical Nutrition*, 76, 5-56.

Goñi, I., Garcia-Alonso, A., & Saura-Calixto, F. (1997). A starch hydrolysis procedure to estimate glycemic index. *Nutrition Research*, 17, 427-437.

Grundy, M. M. L., Edwards, C. H., Mackie, A. R., Gidley, M. J., Butterworth, P. J., & Ellis, P. R. (2016). Re-evaluation of the mechanisms of dietary fibre and implications for macronutrient bioaccessibility, digestion and postprandial metabolism. *British Journal of Nutrition*, 116, 816-833.

Hasjim, J., Cesbron Lavau, G., Gidley, M. J., & Gilbert, R. G. (2010). In vivo and in vitro starch digestion: Are current in vitro techniques adequate. *Biomacromolecules*, 11, 3600–3608.

Hasjim, J., Li, E., & Dhital, S. (2013). Milling of rice grains: Effects of starch/flour structures on gelatinization and pasting properties. *Carbohydrate Polymers*, 92, 682-690.

International Standardization Organization (2011). Determination of amylose content. ISO 6647-2.

Jenkins, D. J. A., Ghafari, H., Wolever, T. M. S., Taylor, R. H., Jenkins, A. L., Barker, H. M., Fielden, H., & Bowling, A. C. (1982). Relationship between rate of digestion of foods and post-prandial glycaemia. *Diabetologia*, 22, 450-455.

Jenkins, D. J. A., Kendall, C. W. C., Augustin, L. S. A., Franceschi, S., Hamidi, M., Marchie, A., Jenkins, A. L., & Axelsen, M. (2002). Glycemic index: Overview of implications in health and disease. *American Journal of Clinical Nutrition*, 76, 266S–73S.

Jiang, H., Horner, H. T., Pepper, T. M., Blanco, M., Campbell, M., & Jane, J. L. (2010). Formation of elongated starch granules in high-amylose maize. *Carbohydrate Polymers*, 80, 533-538.

Juarez-García, E., Agama-Acevedo, E., Gomez-Montiel, N. O., Pando-Robles, V., & Bello-Perez, L. A. (2013). Proteomic analysis of the enzymes involved in the starch biosynthesis of maize with different endosperm type and characterization of the starch. *Journal of the Science and Food Agriculture*, 93, 2660-2668.

Lee, B. H., Bello-Pérez, L. A., Lin, A. H. M., Kim, C. Y., & Hamaker, B. R. (2013). Importance of location of digestion and colonic fermentation of starch related to its quality. *Cereal Chemistry*, 90, 335-343.

Li, E., Dhital, S., & Hasjim, J. (2014). Effects of grain milling on starch structures and flour/starch properties. *Starch-Stärke*, 66, 15-27.

Li, L., Blanco, M., & Jane, J. (2007). Physicochemical properties of endosperm and pericarp starches during maize development. *Carbohydrate Polymers*, 67, 630-639.

Martinez, M. M., Calviño, A., Rosell, C. M., & Gomez, M. (2014). Effect of different extrusion treatments and particle size distribution on the physicochemical properties of

rice flour. *Food and Bioprocess Technology*, 7, 2657-2665. Miller, G. L. (1959). Use of dinitrosalicylic acid reagent for determination of reducing sugar. *Analytical Chemistry*, 31, 426-428.

Morrison, W. R., & Tester, R. F. (1994). Properties of damaged starch granules. IV. Composition of ball-milled wheat starches and of fractions obtained on hydration. *Journal of Cereal Science*, 20, 69-77.

Morrison, W. R., Tester, R. F., & Gidley, M. J. (1994). Properties of damaged starch granules II: crystallinity, molecular order, and gelatinization of ball-milled starches. *Journal of Cereal Science*, 19, 209-217.

Narváez-González, E. D., Figueroa-Cárdenas, J. D., Taba, S., & Rincón-Sánchez, F. (2006). Kernel microstructure of Latin American races of maize and their thermal and rheological properties. *Cereal Chemistry*, 83, 605–610.

Parada, J., & Aguilera, J. (2007). Food microstructure affects the bioavailability of several nutrients. *Journal of Food Science* 72, 21-32.

Perez, S., Baldwin, P. M., Gallant, D. J. (2009). Structural features of starch granules I. In: J. BeMiller, & R. Whistler (Eds.), *Starch. Chemistry and Technology* (pp. 149-192). New York: Academic Press.

Segundo, C., Román, L., Gomez, M., & Martinez, M. M. (2017). Mechanically fractionated flour isolated from green bananas (*M. cavendishii* var. *nanica*) as a tool to increase the dietary fiber and phytochemical bioactivity of layer and sponge cakes. *Food Chemistry*, 219, 240–248.

Shi, L., Li, W., Sun, J., Qiu, Y., Wei, X., Luan, G., Hu, Y., & Tatsumi, E. (2016). Grinding of maize: The effects of fine grinding on compositional, functional and physicochemical properties of maize flour. *Journal of Cereal Science*, 68, 25-30.

- Tran, T. T. B., Shelat, K. J., Tang, D., Li, E., Gilbert, R. G., & Hasjim, J. (2011). Milling of rice grains. The degradation on three structural levels of starch in rice flour can be independently controlled during grinding. *Journal of Agricultural and Food Chemistry*, 59, 3964-3973.
- Varriano-Marston, E., Ke, V., Huang, G., & Ponte, J. (1980). Comparison of methods to determine starch gelatinization of bakery foods. *Cereal Chemistry*, 57, 242-248.
- Vilaplana, F., & Gilbert, R. G. (2010a). Characterization of branched polysaccharides using multiple-detection size separation techniques. *Journal of Separation Science*, 33, 3537–3554.
- Vilaplana, F., & Gilbert, R. G. (2010b). Two-dimensional size/branch length distributions of a branched polymer. *Macromolecules*, 43, 7321–7329.
- Vilaplana, F., Hasjim, J., & Gilbert, R. G. (2012). Amylose content in starches: Towards optimal definition and validating experimental methods. *Carbohydrate Polymers*, 88, 103–111.
- Wang, D., & Eckhoff, S. R. (2000). Effect of broken corn levels on water absorption and steepwater characteristics. *Cereal Chemistry*, 77, 525-528.
- Wang, K., Hasjim, J., Wu, A. C., Henry, R. J., & Gilbert, R. G. (2014). Variation in amylose fine structure of starches from different botanical sources. *Journal of Agricultural and Food Chemistry*, 62, 4443-4453.
- Wolever, T. M. S., Jenkins, D. J. A., Vuksan, V., Jenkins, A. L., Buckley, G. C., Wong, G. S., & Josse, R. G. (1992). Beneficial effect of a low glycaemic index diet in type 2 diabetes. *Diabetic Medicine*, 9, 451–458.

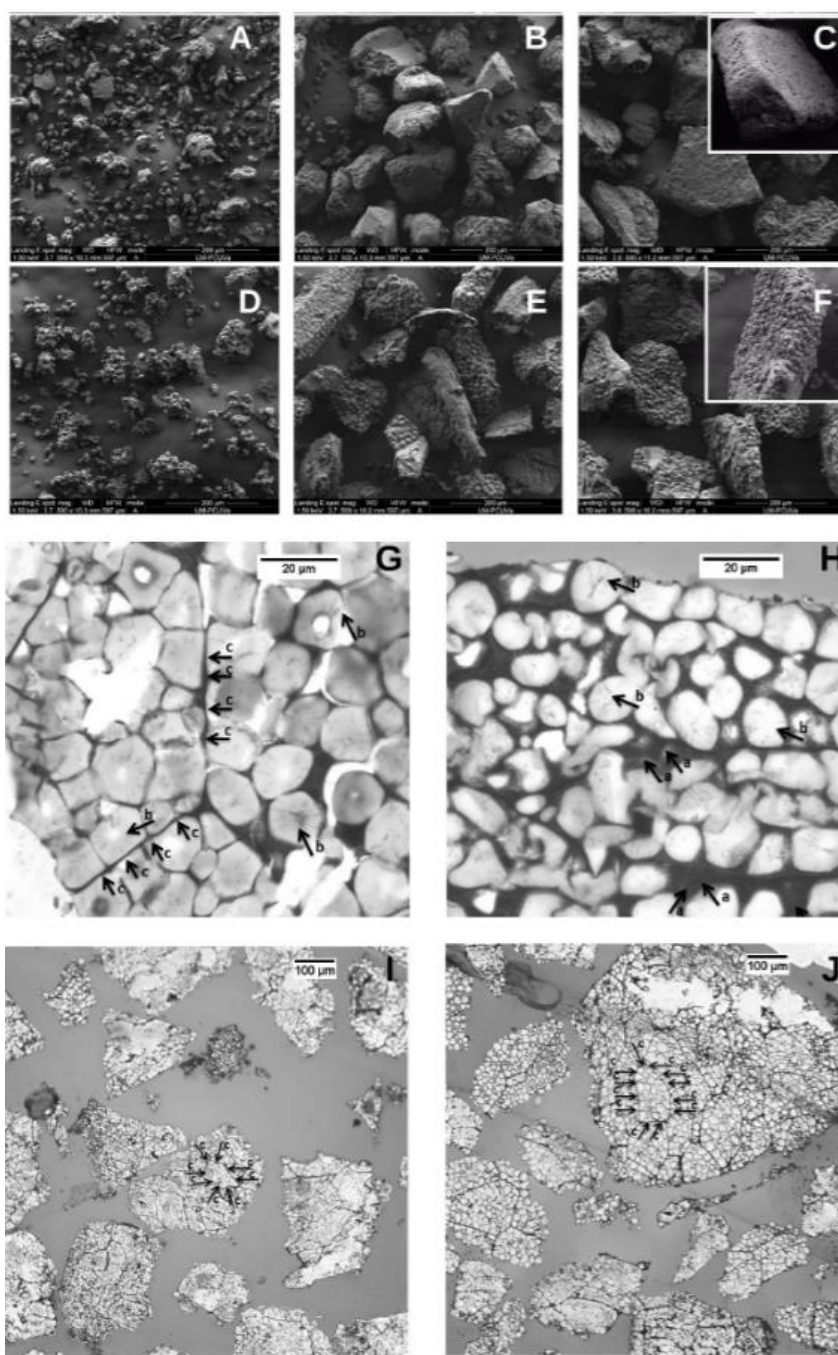


Figure 1. Micrographs of flours from hard and soft endosperm. Environmental scanning electron micrographs (A-F) of hard (A-C) and soft (D-F) with fine (A and D), medium (B and E) and coarse (C and F) particle sizes. Light micrographs (G-J) of the medium fraction from hard (left) and soft (right) endosperm at high (G and H) and low magnification (I and J). Arrows a, b and c represent air pockets, interior channels within starch granules and cell walls, respectively

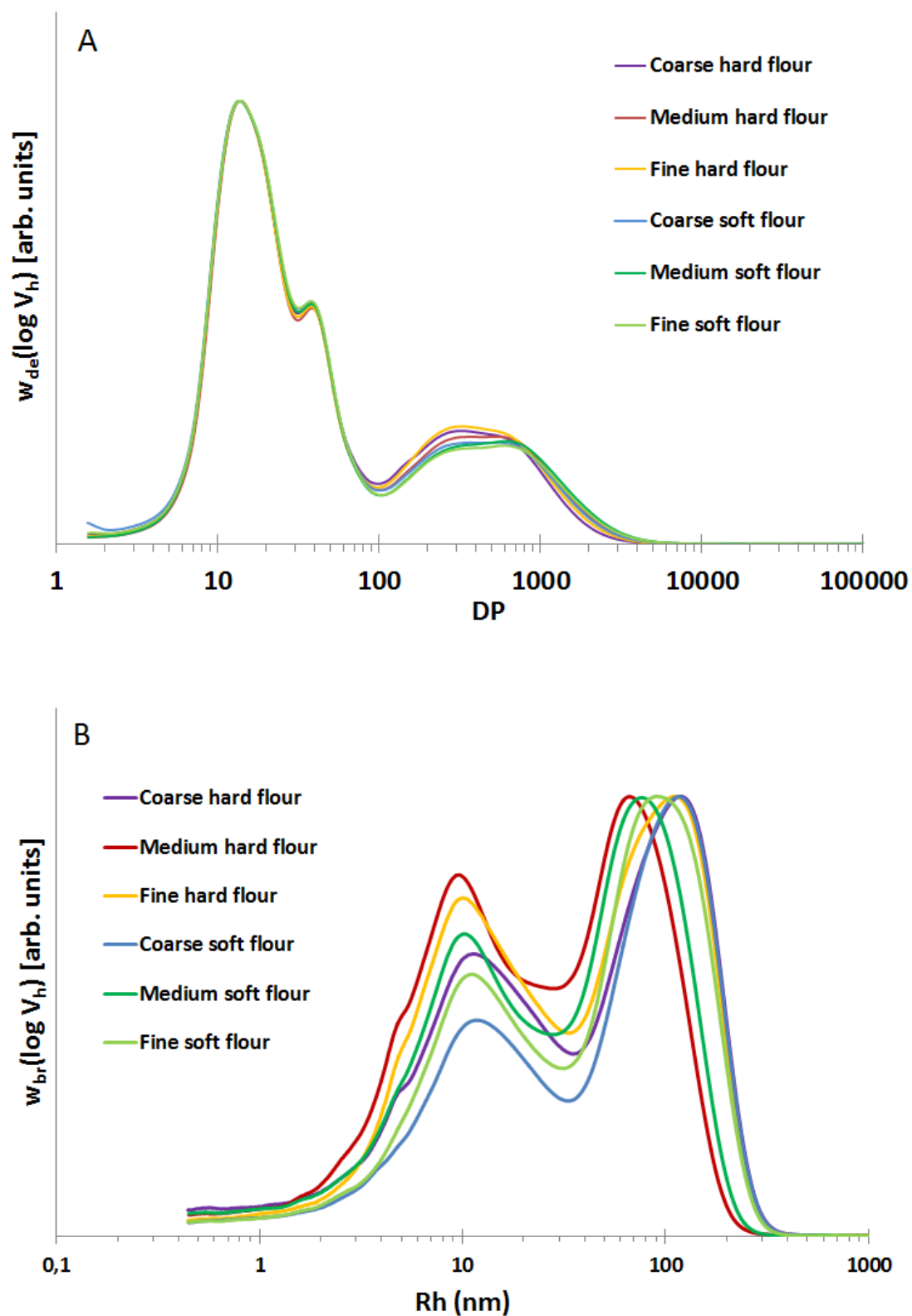


Figure 2. Weight molecular size distributions of enzymatically debranched (A) and fully branched starch (B) of maize flours.

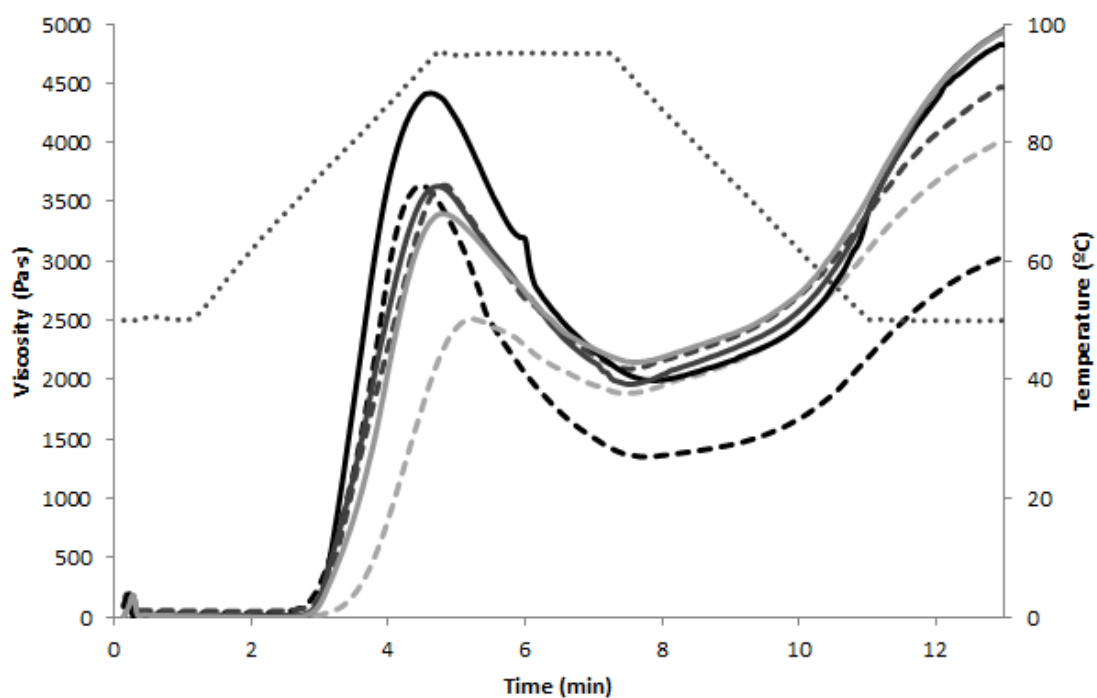


Figure 3. Pasting profiles of fine, medium and coarse fractions from hard (discontinuous line) and soft (continuous line) endosperms. Fine, medium and coarse fractions are presented in black, dark grey and light grey lines, respectively. Temperature profile is represented by dotted line.

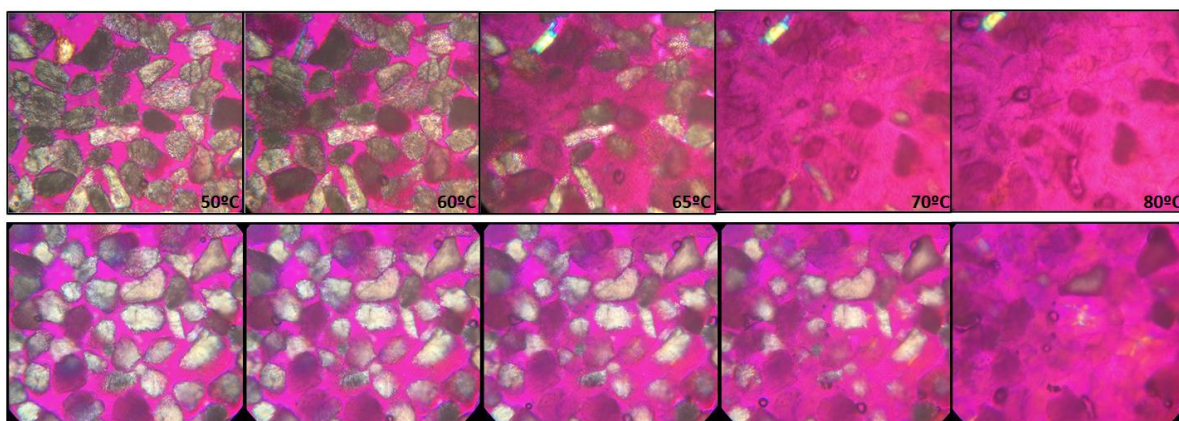


Figure 4. Observations of birefringence (golden-colored particles) and swelling in coarse particles (130-180µm) from soft (upper images) and hard (lower images) endosperm at different temperatures.

Table 1. Damaged starch, amylose content, thermal properties and relative crystallinity of fractions from hard and soft endosperm

Sample	Particle size	Damaged starch (%)	Amylose content (%)	T _o (°C)	T _p (°C)	T _c (°C)	ΔH _g (J/g)	Relative crystallinity (%)
Hard Flours	Coarse	9.22d±0.21	26.85b±0.01	64.31a±0.08	72.75b±0.32	84.26e±0.24	3.55a±0.18	17.52ab±0.5
	Medium	12.09e±0.58	27.46c±0.07	64.50a±1.20	72.60ab±0.7	81.72c±0.31	3.39a±0.29	18.28 abc±0.2
	Fine	14.18f±0.13	27.96d±0.10	64.33a±0.13	71.79a±0.04	80.16a±0.18	3.41a±0.21	15.99a±1.5
Soft Flours	Coarse	4.89a±0.18	25.69a±0.23	65.87b±0.07	72.23ab±0.0	82.93d±0.07	6.01b±0.98	19.92 bc±0.2
	Medium	5.59b±0.03	26.53b±0.12	65.98b±0.21	72.17ab±0.0	81.38c±0.23	5.61b±0.32	23.01d±1.0
	Fine	6.50c±0.17	25.88a±0.41	65.18ab±0.0	71.89ab±0.1	80.77b±0.22	5.44b±0.11	21.25cd±1.0

Values with different letters in the same column are significantly different with $p < 0.05$. Onset (T_o), peak (T_p) and conclusion (T_c) temperatures of gelatinization, ΔH_g= enthalpy of gelatinization

Table 2. Starch fine structure of fractions from hard and soft endosperm

Sample	Particle size	DP of peak maximum in SEC weight molecular size distribution of debranched starch			Height of peak maximum in SEC weight molecular size distribution of debranched starch as ratio to Ap ₁ peak height		Average hydrodynamic radius of whole (fully branched) starch	
		X _{Ap1}	X _{Ap2}	X _{Am}	H _{Ap2/Ap1}	H _{Am/Ap1}	R _{hAm}	R _{hAp}
Hard Flours	Coarse	13.69a±0.03	37.87ab±0.1 ₅	327.68a±11.66	0.543b±0.001	0.257d±0.002	10.35b±0.24	79.42a±6.84
	Medium	13.69a±0.09	38.20b±0.15	364.95a±39.55	0.530a±0.002	0.244c±0.003	9.64a±0.08	66.86a±1.84
	Fine	13.69a±0.03	37.92ab±0.0 ₈	316.95a±3.50	0.534a±0.003	0.264e±0.000	9.66a±0.19	79.57ab±6.8 ₅
Soft Flours	Coarse	13.64a±0.03	37.54a±0.00	486.01b±103. ₈	0.548b±0.002	0.230ab±0.002	11.84d±0.03	115.87c±3.7 ₁
	Medium	13.64a±0.03	38.03b±0.02	608.96c±4.50	0.545b±0.004	0.231b±0.000	10.20b±0.17	76.33ab±5.2 ₂
	Fine	13.69a±0.03	37.98b±0.15	606.92c±13.55	0.545b±0.005	0.225a±0.003	11.12c±0.27	89.85b±8.30

Values with different letters in the same column are significantly different with $p < 0.05$.

Table 3. Effect of flour compactness and particle size on the rate and extent of starch digestion for native and hydrothermally processed samples

Sample	Particle size	Native flours (LOS model)			Hydrothermally processed flours (Goni model)	
		k_1 (min ⁻¹)	k_2 (min ⁻¹)	C_∞ (%)	k (min ⁻¹)	C_∞ (%)
Hard Flours	Coarse	0.118ab±0.009	0.026abc±0.003	53.89b±4.92	0.015a±0.004	115.42b±24.46
	Medium	0.143cd±0.000	0.036c±0.007	57.21b±0.28	0.025bc±0.004	104.80ab±7.02
	Fine	0.161d±0.003	0.033bc±0.000	68.04c±1.73	0.039d±0.006	90.56a±1.01
Soft Flours	Coarse	0.103a±0.012	0.022a±0.001	39.09a±0.90	0.022b±0.002	94.63a±9.47
	Medium	0.105a±0.006	0.023ab±0.009	34.98a±0.52	0.029c±0.001	97.90a±4.70
	Fine	0.132bc±0.001	0.024ab±0.000	35.23a±4.27	0.035d±0.001	90.88a±2.34

Values with different letters in the same column are significantly different with $p < 0.05$.